Molecular Therapy
Nucleic Acids
Original Article

hsa_circ_0092306 Targeting miR-197-3p Promotes Gastric Cancer Development by Regulating PRKCB in MKN-45 Cells

Zihao Chen,[1,2,6] Hongping Ju,[3,4,6] Ting Zhao,[1] Shan Yu,[3] Ping Li,[3] Jing Jia,[3] Nan Li,[3] Xiaojie Jing,[5] Bibo Tan,[2] and Yong Li[2]

[1]Graduate School of Hebei Medical University, Shijiazhuang 050017, Hebei, China; [2]The Third Department of Surgery, The Fourth Hospital of Hebei Medical University, Shijiazhuang 050011, Hebei, China; [3]School of Medicine, Kunming University, Kunming 650214, Yunnan, China; [4]The Respiratory System Disease Prevention and Control of Public Service Platform of Science and Technology in Yunnan Province, Kunming 650214, Yunnan, China; [5]Department of Medicine, The People's Hospital of Economic and Technological Development Zone, Kunming 650217, Yunnan, China

Gastric cancer (GC) is one of the most common cancers worldwide and is thus a global cancer burden. Here, we focused on a novel circular RNA hsa_circ_0092306 and explored the potential molecular mechanism to provide a new target for and novel insights into GC treatment. The GEO microarray was mined and analyzed with R software. Sanger sequencing and RNase R assay were applied to verify the identification of hsa_circ_0092306. Quantitative real-time PCR and western blot were performed to measure the mRNA and protein levels. Pull-down and luciferase reporter assays were conducted to confirm the target relationships. Annexin V-PI apoptosis flow cytometry, 3-(4,5Dimethylthiazol- yl)-2,5Dimethylthiazol-2-yl)-2,5diphenyltetrazolium bromide (MTT), wound healing, and Transwell assays were applied to detect cell apoptosis, viability, migration, and invasion in MKN-45 cells, respectively. A xenograft *in vivo* experiment was conducted to confirm the cell experiment results. hsa_circ_0092306 was upregulated in GC tissues and GC cells, and promoted GC development in MKN-45 cells. hsa_circ_0092306 inhibited tumor suppressor miR-197-3p expression but promoted tumor promotor protein kinase C beta (PRKCB) expression in MKN-45 cells. hsa_circ_0092306 and PRKCB had a common target (miR-197-3p) and were negatively related to miR-197-3p expression. hsa_circ_0092306 promoted the development of GC by regulating the pathway of miR-197-3p/PRKCB in MKN-45 cells.

INTRODUCTION

Gastric cancer (GC) is responsible for a notable proportion of cancer morbidity and mortality worldwide.[1] Globally, stomach cancer is the fifth leading cause of cancer and the third leading cause of cancer-related death. The rate of GC has not decreased in east Asia,[2] although the mortality rates have been decreasing in many areas of the world.[3] Therefore, finding an effective treatment and enhancing understanding of the occurrence and development of GC are necessary.

With the emergence of high-throughput sequencing (also called next-generation sequencing [NGS]), diverse biological components can be uncovered simultaneously.[4] Non-coding RNAs (ncRNAs) have been identified as regulatory factors that are involved in tumor occurrence and progression.[5] Circular RNAs (circRNAs) are a type of ncRNA with a closed annular structure. NGS provides an approach to investigate circRNAs and uncover their functions.[6] circRNAs have a covalently closed continuous loop and are conserved across species because of their resistance to RNase R.[7] Scholars have noted that circRNAs may play an important role in many diseases,[8] especially cancer. For instance, circ_FBXW7 repressed glioma tumorigenesis,[9] circ_cSMARCA5 restrained the growth and metastasis of hepatocellular carcinoma,[10] circ_PRKCI promoted tumor growth in lung adenocarcinoma, and circ_LARP4 inhibited GC.[11] The microRNA (miRNA)-circRNA networks revealed novel insights into the mechanisms underlying the progression and development of malignant tumors.[12] Therefore, finding a functional circRNA in GC and exploring its potential mechanism will be interesting and meaningful.

miRNAs are defined as non-coding, small, single-stranded RNAs that inhibit gene expression post-transcriptionally through sequence-specific interactions with the 3′ UTRs of their cognate mRNA targets.[13] In cancers, miRNAs are always deregulated. These dysregulated miRNAs exert as a group to mark differentiation states or function individually as tumor suppressors or bona fide oncogenes.[14] Dysregulation of miRNAs is associated with tumorigenesis and fibroblast reprogramming in cancer.[15] In the context of GC, recent reports

Received 28 August 2018; accepted 7 August 2019;
https://doi.org/10.1016/j.omtn.2019.08.012.

[6]These authors contributed equally to this work.

Correspondence: Hongping Ju, School of Medicine, Kunming University, No. 2 Puxin Road, Kunming 650214, Yunnan, China.
E-mail: hhjfxdd@126.com
Correspondence: Yong Li, The Third Department of Surgery, The Fourth Hospital of Hebei Medical University, No. 12 Jiankang Road, Shijiazhuang 050011, Hebei, China.
E-mail: hehuiyu02@126.com

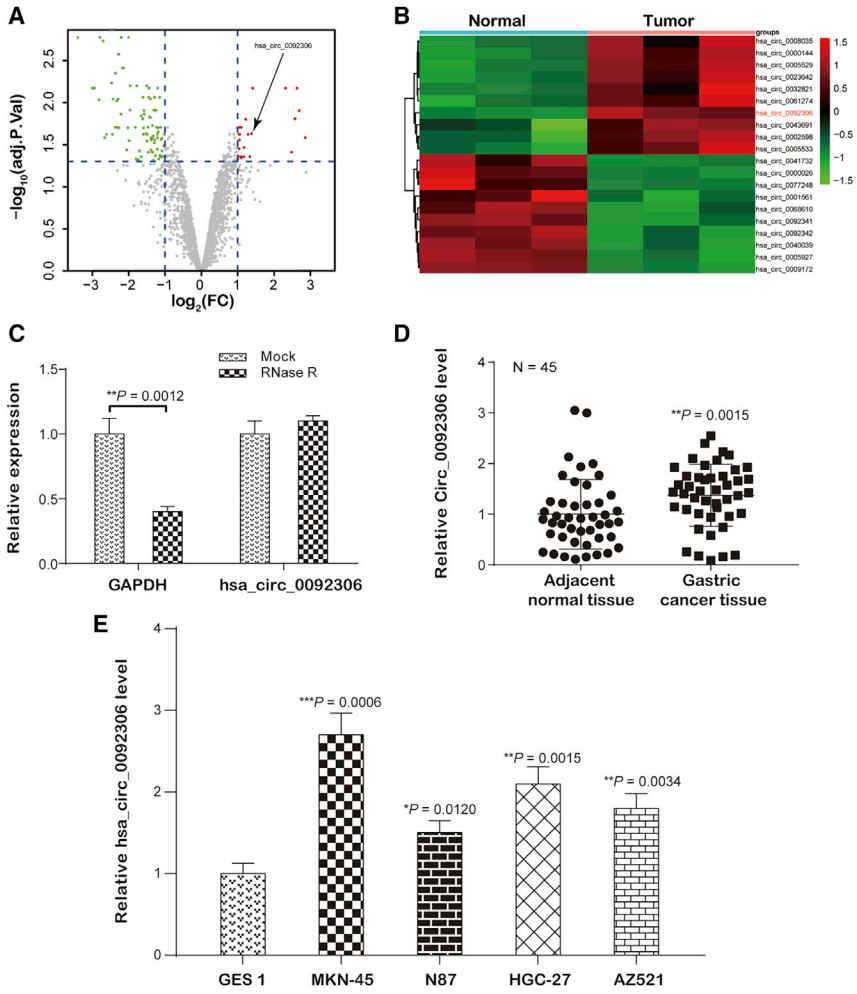

Figure 1. hsa_circ_0092306 Was Upregulated in Gastric Cancer (GC)

(A) Volcano plot of differentially expressed circRNAs. Twenty-two upregulated circular RNAs and 92 downregulated circular RNAs were screened (red: upregulated, green: downregulated). (B) Heatmap showing the top 20 significant disordered circular RNAs in GEO: GSE78092; hsa_circ_0092306 was upregulated in GC tissues. (C) RNase R assay verified the circular RNA identification of hsa_circ_0092306 in GC tissues. (D) hsa_circ_0092306 was significantly upregulated in 45 paired GC and adjacent tissues. (E) Relatively higher expression of hsa_circ_0092306 existed in four GC cell lines (MKN-45, N87, HGC-27, and AZ521) compared with the human gastric mucosa cell (GES 1). *p < 0.05, **p < 0.01, and ***p < 0.001 meant statistical significance.

showed that characteristic miRNA signatures were closely associated with disease progression and clinical outcomes.[16] Moreover, some miRNAs that were altered in GC were verified to control GC cell proliferation, apoptosis, and inflammation.[17] However, the mechanism underlying the deregulation of miRNA expression in GC remains unclear.

Protein kinase C beta (PRKCB) is a gene of a protein kinase C gene family member that codes protein kinase C (PKC) beta-type protein.[18] PKC is a family of serine- and threonine-specific protein kinases that can be activated by calcium and the second messenger diacylglycerol, and serve as major receptors for phorbol esters, which are a class of tumor promoters.[19] Members of the PKC family have peculiar expression trends and are thought to play a unique role in cancer-related processes.[20,21] However, the function of PKC beta 1 in GC has not been reported.

In this study, we performed a microarray analysis and screened out differentially expressed hsa_circ_0092306, which was upregulated in GC. Then, we identified the downstream factors of hsa_circ_0092306 (miR-197-3p and PRKCB) and verified that hsa_circ_0092306 performed a tumor-promotive function that originated in regulation of these two genes. Our findings might provide novel insights for future GC treatment strategies.

RESULTS

circRNA hsa_circ_0092306 Was Upregulated in GC

The expression profile of GSE78092, which contained 6 samples, including 3 GC tissues and 3 normal tissues, was analyzed, and 22 upregulated and 92 downregulated circRNAs were screened out ($p < 0.05$; Figure 1A). hsa_circ_0092306 was one of the top 20 differentially expressed circRNAs and was upregulated in GC tissues compared with its expression in normal tissues ($p < 0.05$; Figure 1B). The University of California Santa Cruz (UCSC) Genome Browser (http://genome.ucsc.edu/) showed that hsa_circ_0092306 originated from human chromosome 11 matured and circled as a 341-bp circRNA (Figure S1). The identification of hsa_circ_0092306 was verified by Sanger sequencing with the ligation sequence 5′-CTAGTTGTTTACGAAACCCCA-3′. RNase R treatment consolidated the identity of hsa_circ_0092306 in GC tissues, because RNase R digests only linear RNA but has no effect on circRNA ($p < 0.05$; Figure 1C). Moreover, hsa_circ_0092306 was expressed at a higher level in the cancer tissues than in the normal cancer tissues ($p = 0.0015$; Figure 1D). Next, hsa_circ_0092306 expression was measured in GC cell lines (MKN-45, MKN7, HGC-27, and AZ521) and the gastric mucosal epithelial cell line GES 1 using quantitative real-time PCR. Similarly, hsa_circ_0092306 was more highly expressed in the GC cell lines than in the gastric mucosal epithelial cells (Figure 1E). Because the hsa_circ_0092306 expression level was highest in the MKN-45 cells, this cell line was selected for the following experiments to verify the function of hsa_circ_0092306 in GC cells.

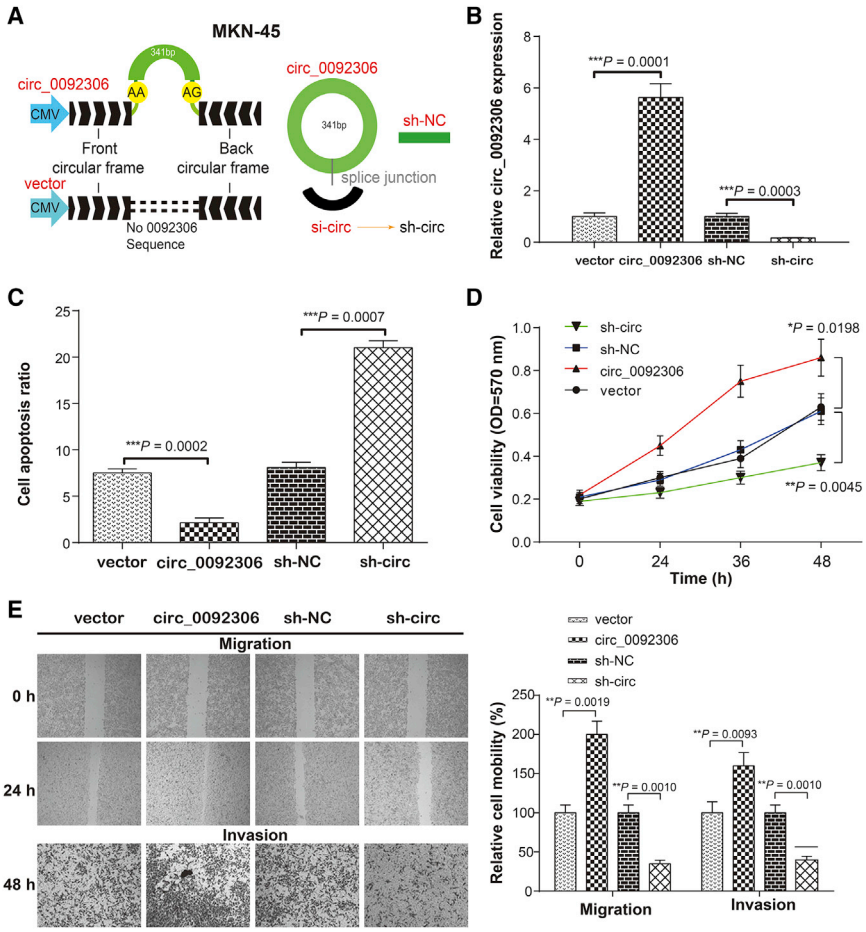

Figure 2. hsa_circ_0092306 Promoted the GC Development in MKN-45 Cells

(A) A schematic diagram of the carrier construction of pLO-ciR used for hsa_circ_0092306 overexpression and pYrbio-LT-1 used for hsa_circ_0092306 knockdown. (B) Successful transfections of hsa_circ_0092306 overexpression and hsa_circ_0092306 knockdown had been verified in MKN-45 cells. (C) Flow cytometry showed a lower apoptosis ratio in the hsa_circ_0092306 overexpression group, which was opposite to that in the hsa_circ_0092306 knockdown group. (D) MTT observed cell viability from 0 to 48 h and revealed robust cell viability in the hsa_circ_0092306-overexpressed group. (E) Wound healing and Transwell assays reflected stranger cell migration and invasion of MKN-45 cells after hsa_circ_0092306 overexpression. *p < 0.05, **p < 0.01, and ***p < 0.001 meant statistical significance.

hsa_circ_0092306 Promoted the Development of MKN-45 Cells

The circRNA overexpression vector of pLO-ciR was used for hsa_circ_0092306 overexpression, and a specific short hairpin RNA (shRNA) targeting hsa_circ_0092306 was transformed into pYrbio-LT-1 plasmid to knock down the hsa_circ_0092306 expression (Figure 2A). An empty pLO-ciR vector or pYrbio-LT-1 containing a shRNA control sequence was regarded as the corresponding negative control. After evaluation of the transfection efficiency, the effects of hsa_circ_0092306 on cell apoptosis, viability, and mobility in MKN-45 cells were evaluated with apoptosis flow cytometry, 3-(4,5Dimethylthiazol- yl)-2,5Dimethylthiazol-2-yl)-2,5diphenyltetrazolium bromide (MTT), wound healing, and Transwell invasion assays (Figures 2B–2E). hsa_circ_0092306 overexpression was accompanied by a lower apoptosis ratio but higher viability and mobility, which were opposite to the results with hsa_circ_0092306 knockdown. Furthermore, the correlation of relative hsa_circ_0092306 expression with the clinicopathological characteristics of 45 patients with GC was analyzed. We found that hsa_circ_0092306 expression was positively related to tumor size, histological grade, TNM stage, and lymph node metastasis ($p = 0.0389$, $p = 0.0307$, $p = 0.0076$, and $p = 0.0027$, respectively; Table S1). Given that hsa_circ_0092306 functions as a tumor suppressor, MKN-45 cells stably transfected with hsa_circ_0092306 knockdown (sh-circ) and negative control circRNA (sh-NC) were subcutaneously injected into the back flanks of nude mice to observe the influence of hsa_circ_0092306 on GC tumor growth *in vivo*. Obviously, the tumors were smaller ($p = 0.0385$; Figures S2A and S2B) and lighter ($p = 0.0102$; Figure S2C) in the sh-circ group than that in the sh-NC group, and the hsa_circ_0092306 expression level was inhibited by sh-circ ($p = 0.0030$; Figure S2D), which indicated a promotional effect of hsa_circ_0092306 on GC development in MKN-45 cells.

PRKCB Was Upregulated in GC and Positively Related to hsa_circ_0092306

According to a previous report,[22] a PRKCB inhibitor (enzastaurin) induces apoptosis in GC cells. Thus, the effects of PRKCB on GC progression were investigated in this study. The expression of PRKCB was higher in GC tissues and had a positive relationship with hsa_circ_0092306 expression (Figures 3A and 3B). Similarly, the mRNA PRKCB and its encoded protein PKC-beta 1 (PKCβ1) expression was upregulated in GC cells (Figure 3C). Moreover, PRKCB expression presented a consistent expression relationship with hsa_circ_0092306 *in vitro* and *in vivo*. In detail, the expression of mRNA PRKCB and protein PKCβ1 was increased in the hsa_circ_0092306 overexpression group and decreased in the hsa_circ_0092306 knockdown group in MKN-45 cells (Figure 3D). *In vivo* assay suggested that the mRNA PRKCB or protein PKCβ1 expression was decreased by the hsa_circ_0092306 downregulation (Figures 3E and 3F).

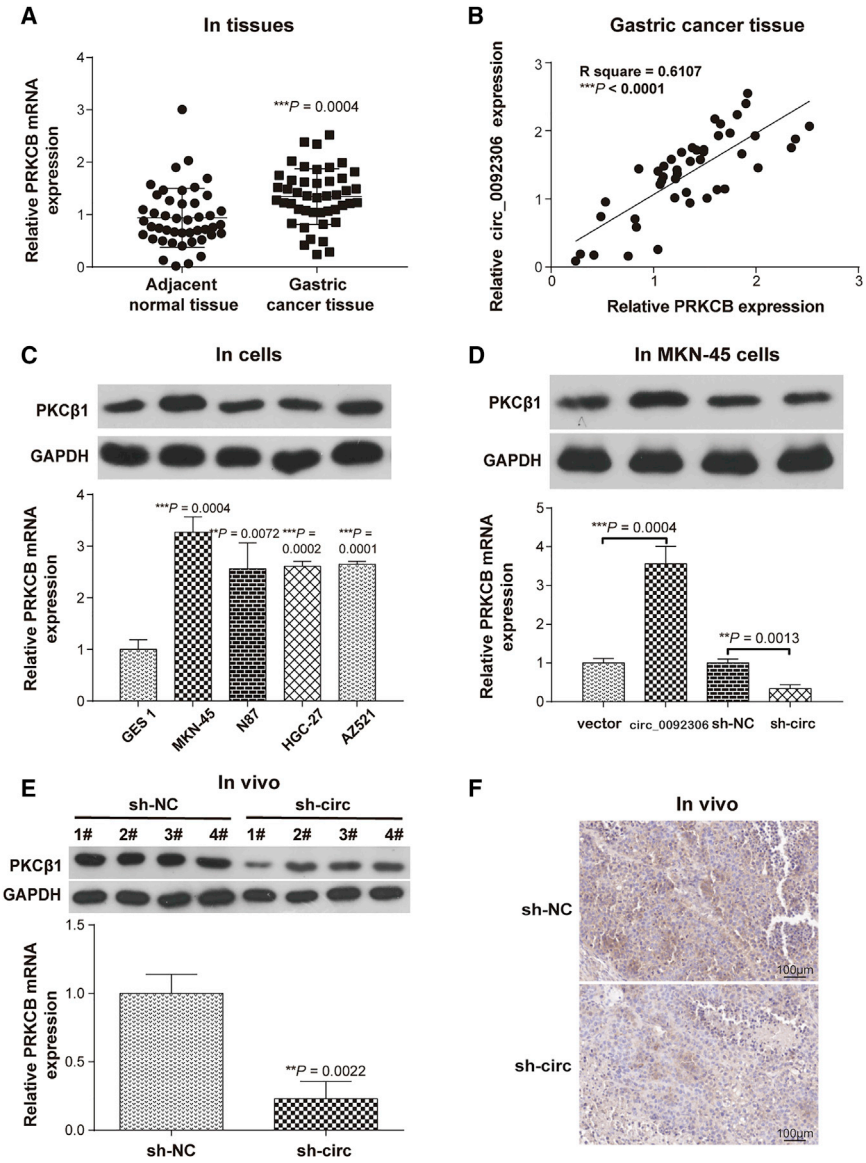

Figure 3. PRKCB Was Upregulated in GC and Positively Related to hsa_circ_0092306

(A) Quantitative real-time PCR showed PRKCB was significantly upregulated in 45 paired GC and adjacent tissues. (B) The PRKCB expression was positively related to the hsa_circ_0092306 expression in 45 GC tissues. (C) The expressions of PKCβ1 protein and PRKCB mRNA in the normal gastric mucosal epithelial cells and GC cells were detected by western blot and quantitative real-time PCR. (D and E) The expressions of PKCβ1 protein and PRKCB mRNA after regulating the hsa_circ_0092306 expression were detected in MKN-45 cells (D) and tumor tissues (E). (F) The expression of PKCβ1 protein after regulating the hsa_circ_0092306 expression was determined by immunohistochemistry. **p < 0.01 and ***p < 0.001 meant statistical significance.

miR-197-3p Targeted hsa_circ_0092306 and PRKCB, and Inhibited the Development of MKN-45 Cells

Given that hsa_circ_0092306 and PRKCB are involved in the occurrence and development of GC, it is interesting whether there is a linker playing a regulatory role between hsa_circ_0092306 and PRKCB. According to Circular RNA Interactome (https://circinteractome.nia.nih.gov/index.html), there are 13 miRNAs targeting hsa_circ_0092306. Based on the data obtained from TargetScanHuman (http://www.targetscan.org/vert_72/), 1,157 miRNAs target PRKCB. In addition, 351 miRNAs shown in the Human microRNA Disease Database (HMDD; http://www.cuilab.cn/hmdd) were associated with GC. As shown in Figure S3A, the intersection of the above three parts contains four miRNAs (miR-197, miR-146b, miR-874, and miR-198). These four miRNAs expressions were detected in GSE 1, MKN-45, and HGC-27 cells, and results showed that only miR-197-3p expression was lower in both MKN-45 and HGC-27 cells than that in GSE 1 cells (Figure S3B). Therefore, miR-197-3p were finally screened out for further studies.

A lower miR-197-3p level was detected in the GC tissues than in the adjacent samples ($p = 0.0002$; Figure 4A) and was negatively associated with hsa_circ_0092306 ($p < 0.0001$; Figure 4B). These findings were supported by the results of the *in vitro* and *in vivo* assays, which showed that hsa_circ_0092306 overexpression inhibited the miR-197-3p expression in MKN-45 cells and the hsa_circ_0092306 knockdown promoted the miR-197-3p expression in MKN-45 cells and *in vivo* assay (Figures 4C and 4D). Similarly, the miR-197-3p expression was negatively related to the PRKCB expression ($p < 0.0001$; Figure 4E). Furthermore, that a target relationship existed between hsa_circ_0092306 and miR-197-3p was confirmed by dual-luciferase reporter experiment and hsa_circ_0092306 probe pull-down assay (Figures 4F and 4G), and that a target relationship existed between miR-197-3p and PRKCB was indicated by dual-luciferase reporter assay (Figure 4H). Only miR-197-3p showed inhibition of the luciferase activity in the wild-type hsa_circ_0092306 or PRKCB group, and miR-197-3p was significantly enriched in the hsa_circ_0092306-probe group, which reflected a direct target relationship between the two factors.

A miR-197-3p mimics or inhibitor was transfected into MKN-45 cells to overexpress or knock down the expression of miR-197-3p, but had no effect on the hsa_circ_0092306 expression (Figures 5A and 5B). Therefore, we speculated that the hsa_circ_0092306 might target miR-197-3p to suppress miR-197-3p expression in GC cells. In addition, miR-197-3p inhibited the development of MKN-45 cells according to the higher cell apoptosis ratio and weaker cell viability and mobility (migration and

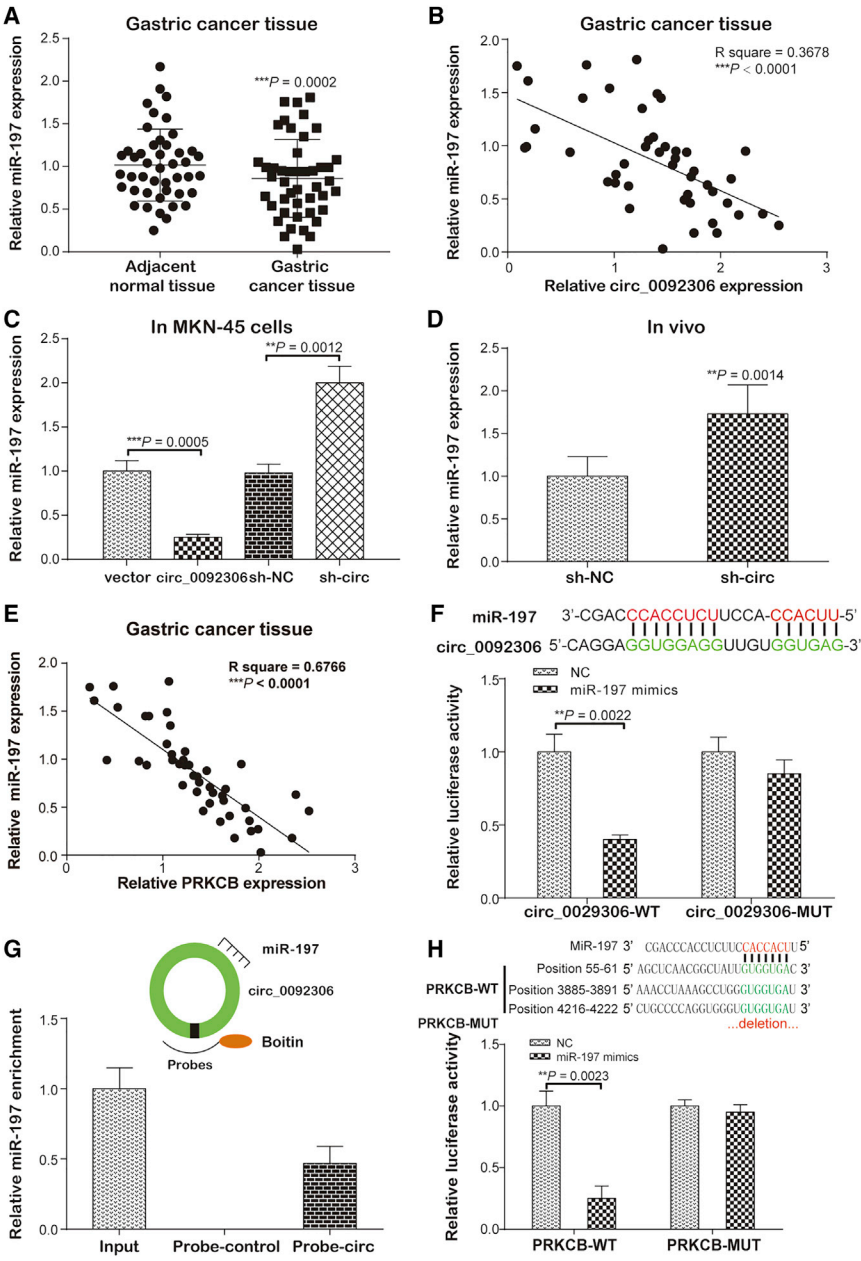

Figure 4. miR-197-3p Targeted hsa_circ_0092306 and PRKCB

(A) Quantitative real-time PCR was performed and showed a lower level of miR-197-3p in 45 paired GC and adjacent tissues. (B) There was a negative relationship between hsa_circ_0092306 and miR-197-3p (R^2 = 0.3678). (C) hsa_circ_0092306 suppressed the miR-197-3p expression in MKN-45 cells. (D) miR-197-3p was upregulated in the hsa_circ_0092306 knockdown tumors. (E) There was a negative relationship between PRKCB and miR-197-3p (R^2 = 0.6766). (F) The targeting sequence between hsa_circ_0092306 and miR-197-3p was revealed by the Circular RNA Interactome, and the luciferase reporter experiment indicated the target relationship of hsa_circ_0092306 and miR-197-3p. (G) miR-197-3p enriched in the pull-down production with the hsa_circ_0092306 probe. (H) The targeting sequence between PRKCB and miR-197-3p was revealed by the TargetScan, and the luciferase reporter experiment indicated the target relationship of PRKCB and miR-197-3p. **p < 0.01 and ***p < 0.001 meant statistical significance.

invasion) in cells transfected with miR-197-3p mimics (Figures 5C–5E). The inhibition of miR-197-3p promoted the development of MKN-45 cells, which could be reversed by the hsa_circ_0092306 knockdown. Therefore, we deduced that hsa_circ_0092306 promoted GC development by targeting miR-197-3p in MKN-45 cells.

PRKCB Was the Downstream Functional Gene of hsa_circ_0092306/miR-197-3p in MKN-45 Cells

The PKCβ1 protein and PRKCB mRNA levels were detected after regulating the expression of miR-197-3p or downregulating the hsa_circ_0092306 expression. The PKCβ1 protein and PRKCB mRNA levels were suppressed by the miR-197-3p mimics and promoted by the miR-197-3p inhibitor, and the promotion induced by the miR-197-3p inhibition was restored by the hsa_circ_0092306 inhibition (Figures 6A and 6B). Moreover, PRKCB overexpression prevented cell apoptosis, improved cell viability, and accelerated cell mobility (migration and invasion), which could be reversed by the hsa_circ_0092306 knockdown or the overexpression of miR-197-3p (Figures 6C and 6E). Meanwhile, the results of *in vivo* assay suggested that PRKCB overexpression promoted tumor growth and PRKCB knockdown inhibited tumor growth, which further confirmed the promotional function of PRKCB on GC progression (Figures S4A and S4B). To prove the relationships among hsa_circ_0092306, miR-197-3p, and PRKCB, hsa_circ_0092306 shRNA and miR-197-3p mimics were injected into the mice treated with PRKCB overexpression tumor for 2 weeks via the tail vein (Figures S4C and S4D). Both hsa_circ_0092306 knockdown and miR-197-3p overexpression could inhibit the overgrowth of tumor caused by the PRKCB upregulation. All of these results showed that hsa_circ_0092306 promoted GC development through regulating the miR-197-3p/PRKCB pathway in MKN-45 cells.

DISCUSSION

Here, we found a 341-bp circular mature RNA derived from chromosome 11 that named hsa_circ_0092306, which had an opposite expression pattern and a target relationship with miR-197-3p in

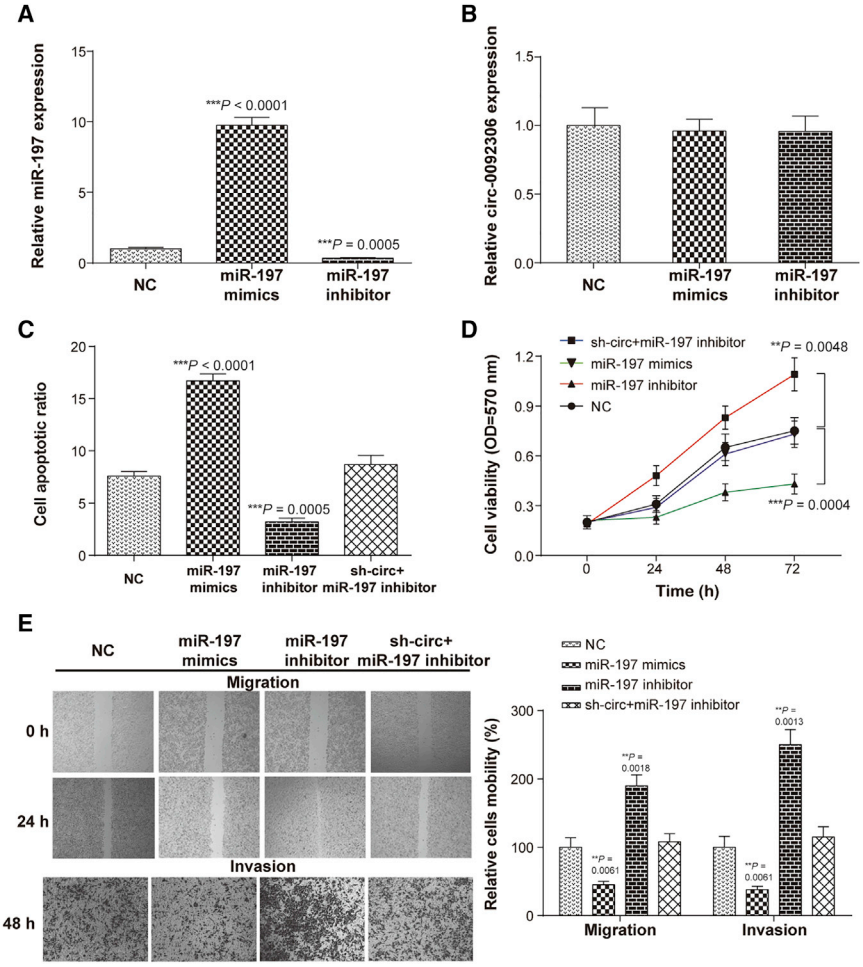

Figure 5. miR-197-3p Inhibited the Development of MKN-45 Cells

(A) miR-197-3p mimics and miR-197-3p inhibitor used to overexpress miR-197-3p or knock down miR-197-3p in MKN-45 cells. (B) miR-197-3p had no effect on hsa_circ_0092306 expression in MKN-45 cells. (C) miR-197-3p promoted cell apoptosis tested with flow cytometry. (D) In MTT assay, miR-197-3p inhibitor enhanced cell viability of MKC-45 cells. (E) Wound healing and Transwell assays suggested weaker cell migration and invasion of MKN-45 cells after miR-197-3p overexpression. **p < 0.01 and ***p < 0.001 meant statistical significance.

GC. hsa_circ_0092306 was upregulated in GC and had a positive function on tumor growth through regulation of the miR-197-3p/PRKCB pathway. This study reports for the first time the promotor function of hsa_circ_0092306 in GC development and the potential molecular mechanism involving targeting miR-197-3p to release PRKCB, which provides a novel treatment target for GC therapy and deepens our understanding of GC growth.

GC is an urgent global problem, especially in China. ncRNAs, including circRNAs, have been shown to regulate the expression of genes involved in the tumor progression of multiple malignancies, including GC.[23] Open public data, such as TCGA and GEO, are convenient for studies. For instance, circLARP4 was found to inhibit GC through miR-424-5p/LATS1,[11] and three upregulated circRNAs were identified as tumor promoters of GC pathogenesis.[24] This study reported that hsa_circ_0092306 was upregulated in GC and promoted GC progression through regulating the miR-197-3p/PRKCB pathway. miR-197-3p was reported to be a tumor suppressor in mass human cancers, such as colorectal cancer,[25] oral squamous cell carcinoma,[26] lung cancer,[27] and prostate cancer;[28] inhibited cell growth and invasion; provided chemo-resistance; and reversed the epithelial-mesenchymal transition.[29–31] Those findings are consistent with our results, which showed that miR-197-3p played an inhibitory role in GC. No study has reported the target relationship between miR-197-3p and PRKCB, which can be viewed as a novel finding in GC. PKCβ1 is encoded by PRKCB and has a complicated function in human cancers. Its inhibition induced apoptosis and inhibited cell-cycle progression.[21] Although PKCβ1 was considered as a suppressor of tumorigenic behavior in pancreatic cancer, PKCβ1-overexpressing cells were more resistant to cell death.[20] Data in this study showed that PKCβ1 overexpression promoted GC cell proliferation and mobility.

Although we explored the function of circRNA 0092306 in GC and the deep underlying mechanism for the first time, our limitations and shortfalls cannot be neglected. The number of clinical samples enrolled in this study is limited, and the results of the association analysis between hsa_circ_0092306 and the clinicopathological characteristics need to be confirmed with larger samples. Possibly not only hsa_circ_0092306 has a function in GC, because the GSE78092 owner noted that hsa_circ_0061274, hsa_circ_0000026, and hsa_circ_0005927 exhibited ectopic expression. Thus, the potential roles of more circRNAs in GC need exploration. Regulation of gene interaction forms an intricate network in cells. The underlying mechanism of miR-197-3p downregulation induced by the overexpression of hsa_circ_0092306 needs to be revealed in future studies. In addition, according to the Circular RNA Interactome website, apart from the miR-197-3p, the tumor suppressors miR-198[32] and miR-383[33] also show a high context with the hsa_circ_0092306 binding score. Similarly, miR-197-3p targets many genes predicted by TargetScan in addition to PRKCB. More research into the mechanism of phosphorylated PRKCB and the downstream signaling pathway in GC should be performed in the future.[34]

First, GEO chips mining showed that hsa_circ_0092306 was abnormally overexpressed in GC, which was verified in GC tissues and cells, and the tumor promotor role of that circRNA and PRKCB was

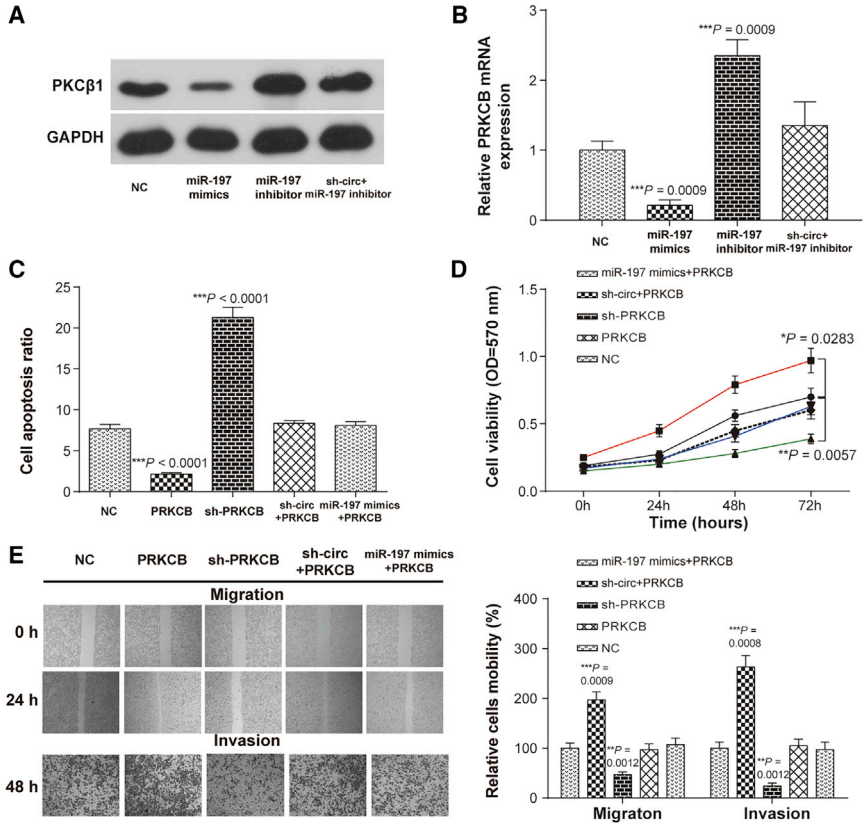

Figure 6. PRKCB Was the Downstream Functional Gene of hsa_circ_0092306/miR-197-3p in MKN-45 Cells

(A and B) The PKCβ1 protein (A) and PRKCB mRNA (B) levels after regulating miR-197-3p or hsa_circ_0092306 in MKN-45 cells were detected by western blot and quantitative real-time PCR, respectively. (C) Flow cytometry showed that PRCKB inhibited cell apoptosis in MKN-45 cells. (D) Cell viability measured by MTT showed a higher cell viability of MKN-45 cells in the PRCKB-overexpressed group. (E) Wound healing and Transwell assays showed higher cell migration and invasion in the PRCKB overexpression group. *p < 0.05, **p < 0.01, and ***p < 0.001 meant statistical significance.

explored *in vitro* and *in vivo*. Second, a target miRNA of hsa_circ_0092306 and PRKCB was revealed with the combination of bioanalysis and experimental verification in GC. Finally, the functional protein PKCβ1-encoded PRKCB gene was found to be downstream of hsa_circ_0092306/miR-197-3p. In conclusion, hsa_circ_0092306 played a promotor role in GC development through inhibiting miR-197-3p expression to increase the expression of PRKCB and its encoded protein PKCβ1, which might provide a novel therapeutic target and potential therapeutic mechanism for GC clinical treatment.

MATERIALS AND METHODS

Bioinformatics Analysis

Data obtained from GSE78092 with the GPL21485 platform were analyzed. Six samples, including three GC tissues and three adjacent normal gastric mucosal tissues, were subjected to ArrayStar Human Circular RNA microarray V2.0 chips analysis. Significant difference in the expression of circRNAs between tumor and adjacent tissues was analyzed by Limma package in the R software with the screening limitation of a $|\log(\text{fold change})| > 1$ and $p < 0.05$. The target relationship between the circRNA and miRNA was analyzed with the Circular RNA Interactome (https://circinteractome.nia.nih.gov/index.html), and the target binding analysis of the mRNA and miRNA was performed with TargetScan (http://www.targetscan.org/vert_72/).

Sanger Sequencing and RNase R Digestion

The hsa_circ_0092396 sequence was obtained using divergent primers sent to Sangon (Shanghai, China) for Sanger sequencing analysis. RNA (5 μg) was incubated for 15 min at 37°C with 3 U/μg of RNase R (Epicenter Biotechnologies, Madison, WI, USA). hsa_circ_0092306 and GAPDH expressions were examined using quantitative real-time PCR after the RNase R digestion reaction.

Tissue Samples

Forty-five paired clinical samples, GC tissues (diagnosed with GC proven by pathological examination) and corresponding cancer adjacent tissues, were collected between August 2015 and December 2018 during radical surgery at The Fourth Hospital of Hebei Medical University. The liquid nitrogen was used to freeze the samples for 5 min, and then the samples were kept at −80°C. The patients did not undergo any treatment, such as chemotherapy, prior to surgery. All patients were provided informed consent for our research.

Cell Culture and Transfection

The human gastric carcinoma cell lines MKN-45, MKN7, HGC-27, and AZ521 and the normal gastric mucosal epithelial cell line GES 1 were all purchased from BNCC (BeNa Culture Collection, Beijing, China). The cell cultures were grown in DMEM supplemented with 10% heat-inactivated fetal bovine serum (FBS), 100 U/mL penicillin, and 100 μg/mL streptomycin (HyClone) in 5% CO_2 and a 37°C humidified atmosphere. The Plasmid vector pLO-ciR (GENESEED, Guangzhou, China) was used for hsa_circ_0092306 overexpression. The plasmid vector pcDNA3.1 used for PRKCB overexpression (PRKCB), miR-197-3p inhibitor, miR-197-3p mimics, and corresponding negative control (vector or NC) were purchased from Thermo Fisher Scientific (Waltham, MA, USA). The pYrbio-LT-1 plasmid (YRBIO, Changsha, China) was used to construct hsa_circ_0092306 knockdown (sh-circ) or PRKCB knockdown (sh-PRKCB) cells. The sh-RNA sequences were provided in Table S2. Lipofectamine 3000 (Invitrogen, Carlsbad, CA, USA) was

applied to carry out cell transfection based on the protocol provided by the manufacturer.

Quantitative Real-Time PCR

Total RNA was extracted from the samples with TRIzol reagent (Invitrogen) transferred into cDNA using ReverTra Ace qPCR RT Kit (Toyobo, Japan). The reverse transcription operation was performed according to the specifications. The reverse transcription products were prepared using THUNDERBIRD SYBR qPCR Mix (Toyobo, Japan) for real-time fluorescent qPCR analysis. GADPH and U6 served as internal controls for the detection of circRNA-mRNA and miRNA, respectively. The primer sequences used for quantitative real-time PCR are provided in Table S3.

Detection of Apoptosis

GC MKN-45 cells were transfected with vehicles as indicated. At 48 h post-transfection, the cell culture medium was replaced with serum-free DMEM. Then, the cells were harvested, washed, re-suspended in the staining buffer, and examined with the Vybrant Apoptosis Assay kit (Invitrogen, Carlsbad, CA, USA). Stained cells were detected with a FACSCalibur, and the data were analyzed with CellQuest software (both from Becton Dickinson, Franklin Lakes, NJ, USA). Annexin V/propidium iodide (PI)-positive cells were regarded as apoptotic cells.

MTT Assay

The cell viability of transfected MKN-45 cells was assessed using the MTT Cell Proliferation Assay Kit (Beyotime, Shanghai, China) in line with the manufacturer's guidance. Transfected MKN-45 cells (5×10^4 per well) were incubated with 10 μL of MTT solution (5 mg/mL prepared with PBS [pH 7.4]) at 37°C for 4 h. Then, stop solution was added to the cells and incubated at 37°C overnight. The optical density value was determined at 570 nm absorbance with the Thermo Scientific Microplate Reader Multiskan MK3 (Thermo Fisher Scientific).

Wound Healing Assay

Transfected MKN-45 cells were grown to 90% confluence in a 24-well plate. Then, a uniform scratch was created with a sterile 10-μL disposable pipette tip. Images of the scraped area were randomly chosen to capture and photograph at 0 and 24 h post-scratch. Meanwhile, the scratch area and the wound healing percentage were analyzed. Three parallel experiments were performed.

Transwell Invasion Assay

In brief, the Transwell upper chamber was coated with 50 μL of Matrigel (BD Biosciences, Franklin Lakes, NJ, USA). The cells (5×10^4) were suspended in 100 μL of serum-free medium and then seeded into the upper floor of Transwell chambers (BD Biosciences). A total of 500 μL of medium with 20% FBS was added to the lower chamber. After 48 h of incubation at 37°C with 5% CO_2, stationary cells were wiped away with a cotton swab, and invasive cells were fixed in methanol and stained with 0.1% crystal violet. The invasive cells were photographed in different fields of view using an inverted phase contrast microscope (CK2; Olympus, Japan).

Tumor Xenografts in Nude Mice

Nude mice at 6–8 weeks of age were purchased from the Experimental Animal Center of the Fourth Hospital of Hebei Medical University, and all animal experiments were approved by the Fourth Hospital of Hebei Medical University animal management center. MKN-45 cells with hsa_circ_0092306 knockdown, PRKCB overexpression, or PRKCB knockdown were constructed and screened through the resistance of the carrier vector. Cells (5×10^6) diluted in 0.1 mL of PBS were subcutaneously injected into the back flank of each mouse. To explore the effect of hsa_circ_0092306, miR-197-3p, and PRKCB on tumor growth *in vivo* and their interrelationships, 200 μm/kg hsa_circ_0092306 shRNA or miR-197-3p mimics was injected (every 3 days) into mice though the tail vein for 2 weeks after PRKCB-overexpressing cells were subcutaneously injected into their back flanks. The tumor size was measured with a caliper every 3 days, and tumor volume was calculated using the formula: Volume = length × width^2 × 0.5. The tumor weight was determined after the mice were sacrificed and the tumors were isolated. At least five mice were included in each group. All experiment procedures were accordance with the ethical manual for laboratory animals.

Dual-Luciferase Assay

The wild-type (WT) PRKCB 3′ UTR or hsa_circ_0092306, which were predicted to target miR-197-3p, or their mutants (MUT) were synthesized, cloned into the psiCHECK-2 vector (Promega, Madison, WI, USA), and co-transfected into 293T cells (BeNa, Beijing, China) with the miR-197-3p mimic or NC using Lipofectamine 3000 (Invitrogen). After 48 h of transfection, luciferase activity was detected with a dual-luciferase assay system (Promega, Madison, WI, USA) based on the manufacturer's instructions.

Pull-Down Assay

A biotin-labeled hsa_circ_0092306 probe (5′-TGA TAT AAC TAG TTG TTT ACG AAA CCC CAT CTC TAC TAA CAA TAC-3′-biotin) was synthesized by Sangon Biotech (Shanghai, China), and the ability of hsa_circ_0092306 to pull down miR-197-3p was assessed. MKN-45 cells were fixed, lysed, and sonicated. After centrifugation, a portion of the supernatant was retained as the input, and the remainder was incubated with a specific hsa_circ_0092306 probe-streptavidin Dynabeads (M-280; Invitrogen) mixture at 30°C overnight. Then, an M-280 Dynabeads-probes-RNAs mixture was washed and incubated with lysis buffer and Proteinase K to reverse the formaldehyde crosslinking, followed by quantitative real-time PCR.

Western Blot Assay

Radio immunoprecipitation assay (RIPA) protein lysis buffer (Beyotime) was applied for protein extraction. After determining the protein concentration using Pierce BCA Protein Assay Kit (Pierce, Rockford, IL, USA), proteins were added to the SDS-PAGE gel and then transferred onto a polyvinylidene fluoride (PVDF) membrane. The membrane was blocked with skimmed milk powder dissolved in TBST for 1 h at room temperature and incubated with primary antibodies (anti-PKCβ1 antibody, ab195039, and anti-GAPDH antibody, ab37168; Abcam, Cambridge, MA, USA) at 4°C overnight.

Subsequently, the membrane was incubated with a secondary antibody (goat anti-rabbit, ab97051; Abcam) for 1 h at room temperature. After washing with TBST, the ECL-PLUS Kit (GE Healthcare, Piscataway, NJ, USA) was applied to visualize the immunoreactive bands in accordance with the kit's instructions.

Immunohistochemistry

Isolated tumor tissues were fixed by formalin, embedded by paraffin, and sliced into 5-μm thickness. Immunochemical staining was carried out according to the standard protocol. The slides were incubated with primary antibody (an anti-mouse monoclonal antibody against PRKCB; Abcam) for 1 h at room temperature, then stained with secondary antibody (biotinylated goat anti-rat immunoglobulin; Abcam) for 30 min at room temperature. Staining intensities of PRKCB were captured under an inverted microscope (Nikon E-800M; Nikon Corporation, Japan) and analyzed using ImageJ software.

Statistical Analysis

All experimental data are presented as mean ± SD. The data were analyzed using one-way ANOVA or Student's t test (GraphPad Prism 6). Linear regression was used to analyze clinical correlations between two genes. Fisher's exact test was applied to analyze the association of hsa_circ_0092306 expression with the clinical characteristics of GC. A p value of less than 0.05 was considered a significant difference.

Ethics Statement and Consent

All procedures performed in studies involving human participants and animals were in accordance with the ethical standards of The Fourth Hospital of Hebei Medical University. Informed consent was obtained from all individual participants included in this study.

SUPPLEMENTAL INFORMATION

Supplemental Information can be found online at https://doi.org/10.1016/j.omtn.2019.08.012.

AUTHOR CONTRIBUTIONS

S.Y., Z.C., and P.L. conceived the research and design. T.Z., H.J., and N.L. analyzed and interpreted data. X.J., B.T., and J.J. analyzed statistics. J.J., Y.L., T.Z., and H.J. drafted the manuscript. Y.L., Z.C., and B.T. critically revised the manuscript. All authors approved the final manuscript.

CONFLICTS OF INTEREST

The authors declare no competing interests.

ACKNOWLEDGMENTS

This study was supported by Kunming Key Laboratory Construction Project (2016-2-A-08038) and Key Projects of Kunming Science and Technology Program (2017-1-S-16405, 2017-1-S-16406, and 2017FH001-083).

REFERENCES

1. Gu, Y., Chen, T., Li, G., Yu, X., Lu, Y., Wang, H., and Teng, L. (2015). LncRNAs: emerging biomarkers in gastric cancer. Future Oncol. *11*, 2427–2441.
2. Siegel, R., Desantis, C., and Jemal, A. (2014). Colorectal cancer statistics, 2014. CA Cancer J. Clin. *64*, 104–117.
3. Yoon, H., and Kim, N. (2015). Diagnosis and management of high risk group for gastric cancer. Gut Liver *9*, 5–17.
4. Caiment, F., Gaj, S., Claessen, S., and Kleinjans, J. (2015). High-throughput data integration of RNA-miRNA-circRNA reveals novel insights into mechanisms of benzo[a]pyrene-induced carcinogenicity. Nucleic Acids Res. *43*, 2525–2534.
5. Huo, L., Zhang, P., Li, C., Rahim, K., Hao, X., Xiang, B., and Zhu, X. (2018). Genome-Wide Identification of circRNAs in Pathogenic Basidiomycetous Yeast Cryptococcus neoformans Suggests Conserved circRNA Host Genes over Kingdoms. Genes (Basel) *9*, e118.
6. Hou, J., Jiang, W., Zhu, L., Zhong, S., Zhang, H., Li, J., Zhou, S., Yang, S., He, Y., Wang, D., et al. (2018). Circular RNAs and exosomes in cancer: a mysterious connection. Clin. Transl. Oncol. *20*, 1109–1116.
7. Qu, S., Zhong, Y., Shang, R., Zhang, X., Song, W., Kjems, J., and Li, H. (2017). The emerging landscape of circular RNA in life processes. RNA Biol. *14*, 992–999.
8. Yang, Z., Xie, L., Han, L., Qu, X., Yang, Y., Zhang, Y., He, Z., Wang, Y., and Li, J. (2017). Circular RNAs: Regulators of Cancer-Related Signaling Pathways and Potential Diagnostic Biomarkers for Human Cancers. Theranostics *7*, 3106–3117.
9. Yang, Y., Gao, X., Zhang, M., Yan, S., Sun, C., Xiao, F., Huang, N., Yang, X., Zhao, K., Zhou, H., et al. (2018). Novel Role of FBXW7 Circular RNA in Repressing Glioma Tumorigenesis. J. Natl. Cancer Inst. *110*, 304–315.
10. Yu, J., Xu, Q.G., Wang, Z.G., Yang, Y., Zhang, L., Ma, J.Z., Sun, S.H., Yang, F., and Zhou, W.P. (2018). Circular RNA cSMARCA5 inhibits growth and metastasis in hepatocellular carcinoma. J. Hepatol. *68*, 1214–1227.
11. Zhang, J., Liu, H., Hou, L., Wang, G., Zhang, R., Huang, Y., Chen, X., and Zhu, J. (2017). Circular RNA_LARP4 inhibits cell proliferation and invasion of gastric cancer by sponging miR-424-5p and regulating LATS1 expression. Mol. Cancer *16*, 151.
12. Bhattacharya, A., and Cui, Y. (2016). SomamiR 2.0: a database of cancer somatic mutations altering microRNA-ceRNA interactions. Nucleic Acids Res. *44* (D1), D1005–D1010.
13. Bartel, D.P. (2009). MicroRNAs: target recognition and regulatory functions. Cell *136*, 215–233.
14. Lujambio, A., and Lowe, S.W. (2012). The microcosmos of cancer. Nature *482*, 347–355.
15. Calin, G.A., and Croce, C.M. (2006). MicroRNA signatures in human cancers. Nat. Rev. Cancer *6*, 857–866.
16. Carvalho, J., van Grieken, N.C., Pereira, P.M., Sousa, S., Tijssen, M., Buffart, T.E., Diosdado, B., Grabsch, H., Santos, M.A., Meijer, G., et al. (2012). Lack of microRNA-101 causes E-cadherin functional deregulation through EZH2 up-regulation in intestinal gastric cancer. J. Pathol. *228*, 31–44.
17. Wu, W.K., Lee, C.W., Cho, C.H., Fan, D., Wu, K., Yu, J., and Sung, J.J. (2010). MicroRNA dysregulation in gastric cancer: a new player enters the game. Oncogene *29*, 5761–5771.
18. Kubo, K., Ohno, S., and Suzuki, K. (1987). Nucleotide sequence of the 3′ portion of a human gene for protein kinase C beta I/beta II. Nucleic Acids Res. *15*, 7179–7180.
19. Dowling, C.M., Phelan, J., Callender, J.A., Cathcart, M.C., Mehigan, B., McCormick, P., Dalton, T., Coffey, J.C., Newton, A.C., O'Sullivan, J., and Kiely, P.A. (2016). Protein kinase C beta II suppresses colorectal cancer by regulating IGF-1 mediated cell survival. Oncotarget *7*, 20919–20933.
20. Cirigliano, S.M., Mauro, L.V., Grossoni, V.C., Colombo, L.L., Diament, M.J., Kazanietz, M.G., Bal de Kier Joffé, E.D., Puricelli, L.I., and Urtreger, A.J. (2013). Modulation of pancreatic tumor potential by overexpression of protein kinase C β1. Pancreas *42*, 1060–1069.
21. Saba, N.S., and Levy, L.S. (2012). Protein kinase C-beta inhibition induces apoptosis and inhibits cell cycle progression in acquired immunodeficiency syndrome-related non-hodgkin lymphoma cells. J. Investig. Med. *60*, 29–38.
22. Lee, K.W., Kim, S.G., Kim, H.P., Kwon, E., You, J., Choi, H.J., Park, J.H., Kang, B.C., Im, S.A., Kim, T.Y., et al. (2008). Enzastaurin, a protein kinase C beta inhibitor, suppresses signaling through the ribosomal S6 kinase and bad pathways and induces apoptosis in human gastric cancer cells. Cancer Res. *68*, 1916–1926.

23. Dang, Y., Ouyang, X., Zhang, F., Wang, K., Lin, Y., Sun, B., Wang, Y., Wang, L., and Huang, Q. (2017). Circular RNAs expression profiles in human gastric cancer. Sci. Rep. *7*, 9060.

24. Lai, Z., Yang, Y., Yan, Y., Li, T., Li, Y., Wang, Z., Shen, Z., Ye, Y., Jiang, K., and Wang, S. (2017). Analysis of co-expression networks for circular RNAs and mRNAs reveals that circular RNAs hsa_circ_0047905, hsa_circ_0138960 and has-circRNA7690-15 are candidate oncogenes in gastric cancer. Cell Cycle *16*, 2301–2311.

25. Lu, X., Liu, Z., Ning, X., Huang, L., and Jiang, B. (2018). The long noncoding RNA HOTAIR promotes colorectal cancer progression by sponging miR-197. Oncol. Res. *26*, 473–481.

26. Ahn, H., Yang, J.M., Kim, H., Chung, J.H., Ahn, S.H., Jeong, W.J., and Paik, J.H. (2017). Clinicopathologic implications of the miR-197/PD-L1 axis in oral squamous cell carcinoma. Oncotarget *8*, 66178–66194.

27. Fiori, M.E., Barbini, C., Haas, T.L., Marroncelli, N., Patrizii, M., Biffoni, M., and De Maria, R. (2014). Antitumor effect of miR-197 targeting in p53 wild-type lung cancer. Cell Death Differ. *21*, 774–782.

28. Daniel, R., Wu, Q., Williams, V., Clark, G., Guruli, G., and Zehner, Z. (2017). A Panel of MicroRNAs as Diagnostic Biomarkers for the Identification of Prostate Cancer. Int. J. Mol. Sci. *18*, e1281.

29. Yang, Y., Li, F., Saha, M.N., Abdi, J., Qiu, L., and Chang, H. (2015). miR-137 and miR-197 Induce Apoptosis and Suppress Tumorigenicity by Targeting MCL-1 in Multiple Myeloma. Clin. Cancer Res. *21*, 2399–2411.

30. Zhang, Y., Li, T., Guo, P., Kang, J., Wei, Q., Jia, X., Zhao, W., Huai, W., Qiu, Y., Sun, L., and Han, L. (2014). MiR-424-5p reversed epithelial-mesenchymal transition of anchorage-independent HCC cells by directly targeting ICAT and suppressed HCC progression. Sci. Rep. *4*, 6248.

31. Hamada, S., Satoh, K., Miura, S., Hirota, M., Kanno, A., Masamune, A., Kikuta, K., Kume, K., Unno, J., Egawa, S., et al. (2013). miR-197 induces epithelial-mesenchymal transition in pancreatic cancer cells by targeting p120 catenin. J. Cell. Physiol. *228*, 1255–1263.

32. Cui, Z., Zheng, X., and Kong, D. (2016). Decreased miR-198 expression and its prognostic significance in human gastric cancer. World J. Surg. Oncol. *14*, 33.

33. Song, Y., Jiang, K., Su, S., Wang, B., and Chen, G. (2018). Clinical manifestations and epigenetic mechanisms of gastric mucosa associated lymphoid tissue lymphoma and long-term follow-up following *Helicobacter pylori* eradication. Exp. Ther. Med. *15*, 553–561.

34. Lau, W.M., Teng, E., Huang, K.K., Tan, J.W., Das, K., Zang, Z., Chia, T., Teh, M., Kono, K., Yong, W.P., et al. (2018). Acquired Resistance to FGFR Inhibitor in Diffuse-Type Gastric Cancer through an AKT-Independent PKC-Mediated Phosphorylation of GSK3β. Mol. Cancer Ther. *17*, 232–242.